


Photonic realization of the κ -deformed Dirac equationP. Majari ^{*}*Instituto de Ciencias Físicas, Universidad Nacional Autónoma de México, Cuernavaca 62210, México*E. Sadurní [†]*Instituto de Física, Benemérita Universidad Autónoma de Puebla, Apartado Postal J-48, 72570 Puebla, México*M. R. Setare[‡]*Department of Science, Campus of Bijar, University of Kurdistan, 6651874871 Bijar, Iran*J. A. Franco-Villafañe [§]*CONACYT-Instituto de Física, Universidad Autónoma de San Luis Potosí, 78290 San Luis Potosí, San Luis Potosí, México*T. H. Seligman^{||}*Instituto de Ciencias Físicas, Universidad Nacional Autónoma de México, Cuernavaca 62210, México
and Centro Internacional de Ciencias, Cuernavaca 62210, México*

(Received 14 December 2020; accepted 12 July 2021; published 23 July 2021)

We show an implementation of a κ -deformed Dirac equation in tight-binding arrays of photonic waveguides. This is done with a special configuration of couplings extending to second-nearest neighbors. Geometric manipulations can control these evanescent couplings. A careful study of wave packet propagation is presented, including the effects of deformation parameters on *Zitterbewegung* or trembling motion. In this way, we demonstrate how to emulate the effects of a flat noncommutative spacetime—i.e., κ -Minkowski spacetime—in simple experimental setups.

DOI: [10.1103/PhysRevA.104.013522](https://doi.org/10.1103/PhysRevA.104.013522)**I. INTRODUCTION**

The field of quantum simulations has been of pivotal importance in the study of physical systems that are experimentally out of reach. Notable examples in cold matter can be found in [1,2] and [3–5] using trapped ions. In this paper, we address the possibility of emulating the effects of Lorentz algebraic deformations on the motion of relativistic electrons [6,7]. In theory, such deformations are associated with a noncommutative geometry of spacetime and a generalized uncertainty principle [8–11]. On physical grounds, the hypothetical corrections stem from a fundamental length scale, which is of a quantum mechanical nature. Let us describe the general features of our proposed emulations to put our work into context. Within the complex quantum simulations class, there are simpler systems whose properties can be studied with single body dynamics. These systems, in turn, can be studied by mesoscopic emulations of quantum mechanical wave equations in microwave [12–17] and photonic experiments [18–25]. We have recently developed a method for simulating position-dependent-mass formalism

of the Dirac equation and Dirac equation in a curved space using waveguide lattices [18]. Such table-top experiments provide flexible configurations and easy tuning of parameters, including recent constructions of effective relativistic systems [26–29]. Examples of condensed matter realizations and their emulations also abound [30–36]. The success of dynamical analogies between quantum mechanical equations and electromagnetic waves in various important subjects—quantum graphs, chaotic scattering and billiards, tight-binding arrays and crystals, including graphene and phosphorene—has led us to consider electromagnetic emulation of the high energy limit of the Dirac equation, ruling the motion of ultrarelativistic fermions. Indeed, Dirac Hamiltonians in 1 + 1 and 2 + 1 dimensions have been produced effectively in a variety of tight-binding systems supported by honeycomb lattices, and in more general settings, by any bipartite (spinorial) lattice entailing Dirac cones in the dispersion relation.

These precedents become important when we look at the so-called κ -deformed algebras at hand [6,7,37,38] and even in the field of q deformations [39,40]. Their effects on quantum field theory have been carefully studied [38,41–47], including particle statistics [48]. In this regard, it has been proved that quadratic corrections in the momentum of a particle will modify the usual Dirac Hamiltonian defined in empty space, even when it represents a physical situation free of interactions [49–51]. As previously mentioned, this is known to take place in the presence of a postulated minimal length, presumably of the order of $G\hbar/c^3 \sim 1.6 \times 10^{-33}$ cm,

^{*}majari@icf.unam.mx[†]sadurni@ifuap.buap.mx[‡]rezakord@ipm.ir[§]jofrabil@ifisica.uaslp.mx^{||}seligman@icf.unam.mx

i.e., the Planck scale. The corresponding corrections would imply a modified energy-momentum relation and extraordinary dispersion relations of matter waves propagating under the effects of new physics. The κ Poincaré Hopf provides us a framework to describe the Planck scale world, and the deformation parameter κ plays the role of Planck mass. On the other hand, noncommutative spacetime is associated with the scale of the spacetime coordinates which is below the Planck scale. κ -Minkowski spacetime has often been suggested as an example of noncommutative spacetime which is invariant under the quantum group of transformations. This paper presents a method for emulating some aspects of the Planck scale world with a macroscopic experiment using an array of microwave resonators [52,53]. In connection with fundamental aspects of physics, some words are in order. Presumably, the existence of a fundamental length is the result of a foamy space consistent with theories that deal with the very nature of spacetime or its emergent properties starting from string theory. However, it is still unknown whether such structures actually underlie our physical world, and it is even more uncertain whether we shall be able to observe the actual consequences of their existence in high-energy experiments or cosmological observations. Important efforts in the phenomenology of deformations and minimal lengths can be found in [54–56], including a plausible stringy origin [57] and Planck scale phenomenology in [58,59]. For this reason, here we recreate the conditions in which the aforementioned effects can be observed. Our aim is to engineer the corresponding dispersion relations with a tight-binding scheme consistent with previous successful emulations of relativistic wave equations. In what touches wave propagation, our emulations shall be able to produce two important effects: (i) a modified energy spectrum in accordance with predictions from potentially new physics and (ii) a corrected evolution of wave packets with modified group velocities in empty space. The first result can be easily achieved by introducing second-neighbor interactions—or hopping amplitudes—in a crystal where Dirac points are initially ensured; this shall be done by simple geometric manipulations of resonators in various realizations, such as optical fibers and ceramic disks. The second result will be tested by a close inspection of a phenomenon known as *Zitterbewegung* [60], already produced artificially in Dirac lattices [1,2,4,61] and calculated in previous treatments [62,63], where some of them cover the full energy band carefully [64]. This reaches well beyond the conical region of the emulated spectrum. With our treatment, we shall be able to compare the oscillation frequency of a wave packet's width—as well as its decay in amplitude—with the expected theoretical predictions, finding, significant effects coming from a hypothetical minimal length, together with corrected trajectories of electrons obtained as average positions in the κ -deformed Heisenberg picture.

The structure of the paper is as follows. In Sec. II, we revisit the emergence of the κ -deformed Dirac equation and obtain the first corrections in the Dirac Hamiltonian due to a fundamental length a . In Sec. III, we present a careful construction of arrays made of coupled optical fibers disposed in a strip resembling a triangular lattice, fulfilling thus a Dirac-like dynamical equation with conical points. In Sec. IV, we study the effects of the deformation on the trembling motion of wave

packets, including the corrections in the width coming from the fundamental length a . A detailed full-band computation of *Zitterbewegung* for tight-binding arrays with second neighbors is offered within Sec. IV. We conclude in Sec. V.

II. THE κ -DEFORMED DIRAC EQUATION

Noncommutative (NC) geometry was envisaged by Gelfand when he showed that a space is determined by the algebra of the functions acting on it. The notion of space is then tied to the nature of its algebra; therefore, a noncommutative spacetime (NCST) follows from a noncommutative algebra. This has been extensively studied in the framework of Hopf algebras and the so-called quantum groups [38,41,42]. In our case, the coordinate functions x_μ satisfy the commutation relations of the form

$$[x_\mu, x_\nu] = i(\Theta_{\mu\nu} + \Theta_{\mu\nu}^\lambda x_\lambda + \dots) = i\Theta_{\mu\nu}(x), \quad (1)$$

which is a relation that has been instrumental in the construction of a deformed quantum field theory [43]. Among all the possible ways of representing NCST, we are particularly interested in the κ -Minkowski spacetime employed in [43–46]. In other words, the κ -Minkowski spacetime is a Lie algebraic deformation of the usual Minkowski (flat) spacetime where the deformation parameter can be related to a length scale in which quantum gravity might take place. The corresponding κ -Poincaré-Hopf algebraic relations can be written in terms of a deformation parameter $\kappa = 1/|a|$, as

$$[\hat{x}_\mu, \hat{x}_\nu] = i(a_\mu \hat{x}_\nu - a_\nu \hat{x}_\mu). \quad (2)$$

Moreover, the existence of such a fundamental scale can be encoded in Dirac operators acting on spinor fields. The deformed Dirac equation obtained in the framework of the κ -Poincaré-Hopf algebra and its equivalent in periodic arrays of coupled waveguides will be studied in the following section. Let us start with the algebra related to NC spaces satisfying the following relations [49,50]:

$$[M_{i0}, \hat{x}_0] = -\hat{x}_i + iaM_{i0}, \quad (3)$$

$$[M_{i0}, \hat{x}_j] = -\delta_{ij}\hat{x}_0 + iaM_{ij}. \quad (4)$$

Here the structure $M_{\mu\nu}$ contains the rotation and boost generators of the κ -Poincaré algebra and \hat{x}_μ denotes the NC coordinates. This algebraic structure also entails the following relations:

$$[\hat{x}_\mu, \hat{x}_\nu] = iC_{\mu\nu\lambda}\hat{x}^\lambda = i(a_\mu \hat{x}_\nu - a_\nu \hat{x}_\mu), \quad (5)$$

where the structure constants are written in terms of a vector Minkowski a_μ and the flat metric $\eta_{\mu\nu}$: $C_{\mu\nu\lambda} = a_\mu \eta_{\nu\lambda} - a_\nu \eta_{\mu\lambda}$. In some frame of reference, $a_i = 0$, $a_0 = a$, and $\hat{x}_i = x_i \phi$ where ϕ is so far free. In the κ -Poincaré algebra, the modified derivative operators D_μ , the so-called Dirac derivatives, are given by [38,42]

$$D_0 = \partial_0 \left(\frac{\sinh(A)}{A} \right) + \frac{ia\nabla^2 e^{-A}}{2\phi^2} \quad (6)$$

and

$$D_i = \partial_i \left(\frac{e^{-A}}{\phi} \right), \quad (7)$$

with $A = -ia\partial_0$ and $a = \kappa^{-1}$. This leads to the following relations [48]:

$$[M_{\mu\nu}, D_\lambda] = \eta_{\nu\lambda}D_\mu - \eta_{\mu\lambda}D_\nu, \quad (8)$$

$$[D_\mu, D_\nu] = 0, \quad (9)$$

where the metric's signature convention is fixed as $\eta_{\mu\nu} = \text{diag}(-1, 1, 1, 1)$. Thus, the deformed Dirac equation is now postulated in terms of D_μ as

$$[i\gamma^\mu D_\mu + m]\psi = 0, \quad (10)$$

where γ^μ are the usual gamma matrices. With the special choice $\phi = e^{-A}$, we eliminate the deformation in the spatial derivatives, leaving us only with a new (corrected) time component D_0 . We note here that this choice, together with the definition of A , turns ϕ into a nonlocal operator in time. By substituting (6) and (7) in the above equation and after a few straightforward manipulations, the following κ -Dirac equation is deduced:

$$\left[i\gamma^0 \left(\frac{i}{a} \sinh(A) + \frac{ia}{2} \nabla^2 \right) + i\gamma^i \partial_i + m \right] \psi = 0, \quad (11)$$

which is written in natural units $\hbar = c = 1$. This equation is, in fact, nonlocal due to the obvious relation $\phi\psi(t) = \psi(t + ia)$ for any wave function ψ . On physical grounds, we may take only the first corrections in a with the aim of describing a slightly perturbed Dirac operator (note, however, that this concession is not made on mathematical grounds because infinite order differential equations cannot be truncated without dire consequences on the oscillatory behavior of their solutions) leading to

$$\left[i\gamma^0 \left(\partial_0 + \frac{ia}{2} \nabla^2 \right) + i\gamma^i \partial_i + m \right] \psi = 0. \quad (12)$$

It follows from the above equation that the corresponding Hamiltonian is

$$H = \alpha \cdot p + \frac{a}{2} \nabla^2 + m\beta, \quad (13)$$

where $p = -i\partial_i$ is the particle momentum. Here, the explicit representation of Dirac matrices in 1 + 1 dimensions given by $\alpha_1 = \sigma_1$ and $\beta = -\sigma_3$ is possible and it is consistent with our choice of metric signature. It is also obvious that the undeformed Dirac equation is obtained in the limit $a \rightarrow 0$. However, we underscore the fact that experimentally, the deformation parameter a is greatly limited by an upper bound of the order of $a < 10^{-29}$ m [31]. Several effects can be investigated using this new Hamiltonian. It might well be that the presence of a modifies the spectrum of a relativistic particle, but it is not easy to gain access to such energy scales in accelerators. There are other effects that could be amplified in other settings, e.g., wave-packet evolution. We shall explore this possibility in the following sections.

III. AN ARRAY OF PHOTONIC WAVEGUIDES

The tight-binding model of the κ -deformed Dirac equation can be implemented on a macroscopic experiment using an array of microwave resonators. The resonators can be built as cylinders of the same size, but with two different dielectric

constants, for example, Exxilia Temex Ceramics E2000 and E3000 with $\epsilon = 36$ and 34, respectively. An induced mass parameter α around 0.28 GHz is expected for cylinders of 8 mm diameter, and their length much larger than their diameter. The nearest-neighbor coupling parameter between the cylinders can be set between 0.4 and 1 GHz, depending on the separation between cylinders. With those experimental parameters, it is possible to estimate the *Zitterbewegung* (ZB) characteristic frequencies ω' and ω . The corresponding oscillation lengths that we named here, λ' and λ , respectively, will be of the order of $\lambda' \sim \text{cm}$ and $\lambda \sim \text{m}$. Those scales make the effect observable on a macroscopic scale, thanks to our tight-binding representation of the corresponding wave operator. In order to excite the resonators, we propose to use an array of antennas. Each antenna will be placed near the end of each fiber or cylinder. The antennas should all be parallel and oriented in such a way that they are capable of exciting an electric field perpendicular to the optical axis and to the horizontal axis. The array of antennas has to be excited by the same microwave frequency but, at the same time, allowing the control of the input power independently in each antenna. One possible and inexpensive way to feed the antennas is to use a direct digital synthesizer (DDS) that provides independent frequency, phase, and amplitude control on each channel.

Another possible way to implement the κ -deformed Dirac equation is through waveguide arrays. In the following, we focus on the correspondence between the disordered waveguide arrays as shown in Fig. 1 and the κ -deformed Dirac equation. The propagation of an optical field of disordered waveguide arrays by using the tight-binding approximation is given by

$$i \frac{dE_n}{dz} + (-1)^n \alpha E_n + C_{n-2} E_{n-2} + C_n E_{n+2} + C'_n E_{n+1} + C'_{n-1} E_{n-1} = 0, \quad (14)$$

where $E_n \equiv E(n, z)$ is the electric field amplitude at the n th waveguide and $C_{n\pm i}$ ($C'_{n\pm i}$) denotes the next-nearest-neighbor coupling (nearest-neighbor coupling). Next, we let upper

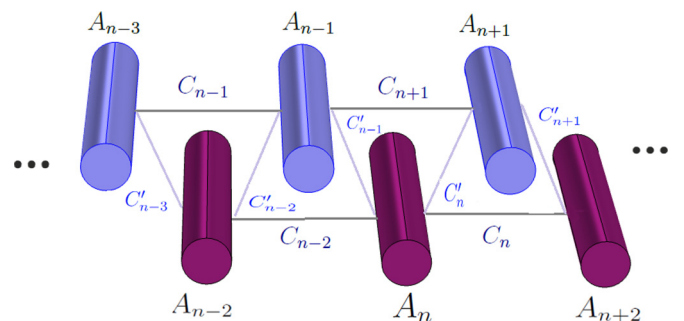


FIG. 1. Schematic view of a binary array made of two types of waveguides, A and B , arranged in a triangular lattice along a strip.

waveguide array have odd numbers. Then,

$$i \frac{dE_{2n}}{dz} + \alpha E_{2n} + C_{2n-2} E_{2n-2} + C_{2n} E_{2n+2} + C'_{2n} E_{2n+1} + C'_{2n-1} E_{2n-1} = 0, \tag{15}$$

and let the lower array label be even ones:

$$i \frac{dE_{2n-1}}{dz} - \alpha E_{2n-1} + C_{2n-3} E_{2n-3} + C_{2n-1} E_{2n+1} + C'_{2n-1} E_{2n} + C'_{2n-2} E_{2n-2} = 0. \tag{16}$$

Now by setting $E_{2n} = (-1)^n \psi_1(n, z) \equiv (-1)^n \psi_1(n)$ and $E_{2n-1} = -i(-1)^n \psi_2(n, z) \equiv -i(-1)^n \psi_2(n)$, Eqs. (15) and (16) can be written as

$$i \frac{d\psi_1(n)}{dz} + \alpha \psi_1(n) - C_{2n-2} \psi_1(n-1) - C_{2n} \psi_1(n+1) + i C'_{2n} \psi_2(n+1) - i C'_{2n-1} \psi_2(n) = 0 \tag{17}$$

and

$$i \frac{d\psi_2(n)}{dz} - \alpha \psi_2(n) - C_{2n-3} \psi_2(n-1) - C_{2n-1} \psi_2(n+1) + i C'_{2n-1} \psi_1(n) - i C'_{2n-2} \psi_1(n-1) = 0. \tag{18}$$

It is straightforward to show that by considering $C_{2n\pm i} = \eta$ and $C'_{2n-i} = \xi$ with $i = 0, 1, \dots$, these equations reduce to

$$i \frac{d}{dz} \begin{bmatrix} \psi_1(n) \\ \psi_2(n) \end{bmatrix} = \begin{bmatrix} -\alpha \psi_1(n) + \eta \psi_1(n-1) + \eta \psi_1(n+1) - i \xi \psi_2(n+1) + i \xi \psi_2(n) \\ +\alpha \psi_2(n) + \eta \psi_2(n-1) + \eta \psi_2(n+1) - i \xi \psi_1(n) + i \xi \psi_1(n-1) \end{bmatrix} = H \begin{bmatrix} \psi_1(n) \\ \psi_2(n) \end{bmatrix}. \tag{19}$$

After the formal change $z \rightarrow t$, the Hamiltonian operator is defined as follows:

$$H = \begin{bmatrix} -\alpha + \eta T^{-1} + \eta T & -i \xi T + i \xi \\ -i \xi + i \xi T^{-1} & \alpha + \eta T^{-1} + \eta T \end{bmatrix}, \tag{20}$$

where T is the translation operator in one unit of n . In order to reduce the system of equations to a 2×2 matrix, we must note that in the case of Bloch wave transport inside the fibers, the wave function must be written in the form $[\psi_1(n, z), \psi_2(n, z)]^\dagger = [A(z)e^{ikn}, B(z)e^{ikn}]^\dagger$, which satisfies Bloch's theorem $T e^{ikn} = e^{ik(n+1)}$. Now, the Hamiltonian (20) is reduced to

$$H = \begin{bmatrix} -\alpha + 2\eta \cos(k) & -i \xi e^{ik} + i \xi \\ -i \xi + i \xi e^{-ik} & \alpha + 2\eta \cos(k) \end{bmatrix} \simeq \begin{bmatrix} -\alpha + 2\eta - \eta k^2 & \xi k \\ \xi k & \alpha + 2\eta - \eta k^2 \end{bmatrix}. \tag{21}$$

Therefore, the energy eigenvalues are given by

$$E = 2\eta \cos(k) + s \sqrt{4\xi^2 \sin^2\left(\frac{k}{2}\right) + \alpha^2}, \tag{22}$$

where $s = \pm 1$. This equation has to hold even beyond the Dirac (conical) points. The eigenfunctions are two-component spinors of the form

$$\begin{pmatrix} u_1 \\ u_2 \end{pmatrix} = \frac{1}{\sqrt{2[E - 2\eta \cos(k)]}} \begin{pmatrix} \sqrt{E - \alpha - 2\eta \cos(k)} \\ e^{-ik/2} \sqrt{E + \alpha - 2\eta \cos(k)} \end{pmatrix}. \tag{23}$$

By setting $k \rightarrow p_x$, the Hamiltonian (21) reduces to the simpler one,

$$H = -\eta p_x^2 I_2 + \xi p_x \sigma_x - \alpha \sigma_z + 2\eta I_2 = H_0 + V, \tag{24}$$

where $V = 2\eta$ is a constant potential, and therefore irrelevant in the dynamics. Finally, we note that after the formal change $\frac{\alpha}{2} \rightarrow \eta$, $m \rightarrow \alpha$, and $1 \rightarrow \xi$, the expression for the Hamiltonian in (13) can be mapped to H_0 previously written in (24).

IV. EVOLUTION OF POSITION IN κ -DEFORMED DIRAC THEORY

Now we would like to investigate one of the special features of the Dirac equation: the trembling motion known as *Zitterbewegung*. To clarify this effect in the κ -Dirac equation, we must calculate the time evolution of the position operator under the strict conditions $\eta \neq 0$, $\alpha \neq 0$. In the absence of rest mass (Weyl equation), we know that there is no visible effect, for the evolution of x would be trivial. The calculation of $x(t)$ for the more general case $\alpha \neq 0$ for the Hamiltonian (24) is, however, straightforward and we shall proceed in this direction. In the Heisenberg picture, we have [31]

$$x(t) = x(0) - 2\eta p_x t + \xi p_x (H')^{-1} t + \frac{i\xi}{2} H'^{-1} [\sigma_x - \xi p_x (H')^{-1}] (e^{-2iH't} - 1), \tag{25}$$

where

$$H' = -\alpha \sigma_z + \xi \sigma_x p_x. \tag{26}$$

To see the dependence on the deformation parameter more clearly, we focus now on the width of the wave packets, $(\Delta x)^2 = \langle x \rangle^2 - \langle x^2 \rangle$. Due to Ehrenfest's theorem, the time average $\langle x \rangle$ suffers the same modifications as the classical trajectory of a particle governed by a κ -deformed energy momentum relation. On the other hand, the second term $\langle x^2 \rangle_\psi$ provides an important modification to the wavelike behavior of the particle. Its explicit form is given by

$$\langle x^2 \rangle_\psi = e^{-\frac{\pi}{10}} \alpha^2 \omega' + e^{\frac{\pi}{10}} (\xi^2 \omega' + 12\eta^2 \omega'^2 - 4\alpha \eta \xi \omega') t^2 - 4e^{-\frac{\pi}{10}} \sqrt{\frac{\pi t}{\vartheta}} \left[-\eta \alpha^2 \pi^2 \xi \sin(2\omega' t) + \frac{\eta \pi \alpha \sqrt{\omega'^2 - \alpha^2}}{\omega'^2} \cos(2\omega' t) \right], \tag{27}$$

as shall be derived later on.

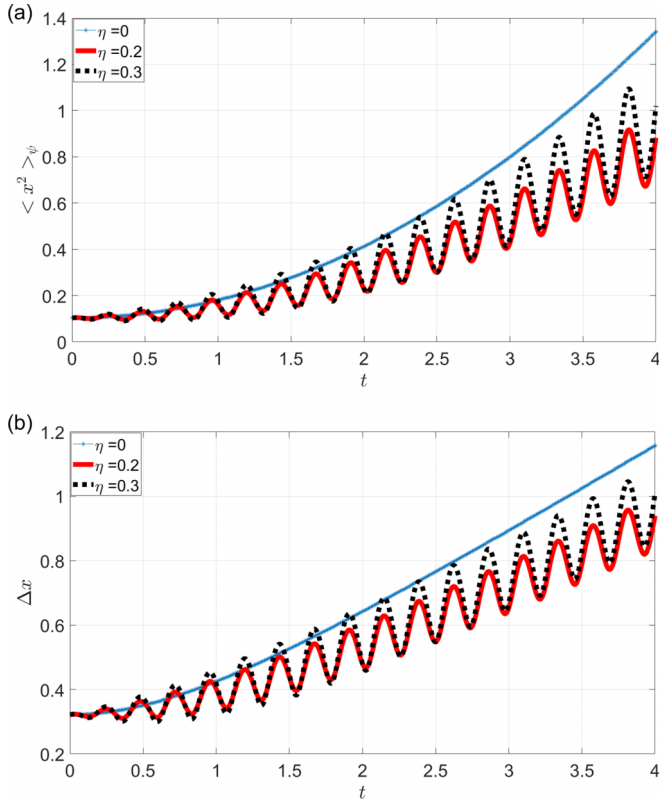


FIG. 2. Time development of (a) $\langle x^2 \rangle_\psi$ and (b) standard deviation, which are plotted in natural units for fixed values $\xi = \alpha = 4$ and different values of η .

The time development of $\langle x^2 \rangle_\psi$ and standard deviation, with $x(0) = 1.5$ and initial width 0.8, are shown in Fig. 2. The interesting effect that has been obtained consists of a deformation-dependent evolution of a particular component in the width contributing to the usual ballistic expansion. As shown in Fig. 2(a), the time development of $\langle x^2 \rangle_\psi$ grows with t^2 and is independent of the damping term with the envelope $1/\sqrt{t}$, which appears in $\langle x \rangle_\psi$ (see the following section). Indeed, the envelopes \sqrt{t} and t^2 are affected by η in the second and third terms of expression (27). This direct proportionality in the third term amplifies the phenomenon in time, but in the case of realistic values of η within experimental bounds, it would be too challenging to detect the correction in experiments with electrons. In general, we can appreciate, in Fig. 2(b), that the packet width exhibits oscillations and the wave packet spread in position increases with η . It is remarkable that the $t^{(-1/2)}$ term appears in the standard deviation, but it does not show in the figure as it is only relevant for very short times and, for the range of η selected in view of the proposed experiment, is overcome by the other terms. In optical realizations, the parameter η is at our disposal, with recommended values shown in the inset of Fig. 2(b), for a better appreciation.

Zitterbewegung in the photonic lattice: Computations

We derive the time evolution of the position operator for photonic waveguide arrays. It is important to do so without

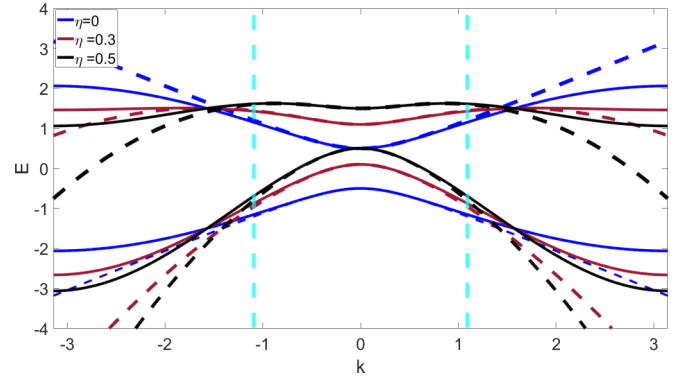


FIG. 3. A comparison of the dispersion relations for waves governed by our tight-binding array (solid lines) and the κ -deformed Dirac equation in natural units (dashed lines). Mass $\alpha = 0.5$, coupling $\xi = 1$. There is good agreement near the Dirac point at $k = 0$. Deformation parameters: $\eta = 0$ (blue), 0.3 (red), and 0.5 (black). The tight-binding relation displays new points of vanishing group velocity in the upper band, marked by light-blue vertical lines. The phase factors, however, cancel out in the computation of averages.

approximations in the tight-binding dispersion relations for an honest comparison with deformed theories. Since the stationary phase approximation will be required in the derivation of averages, it is important to analyze the energy landscape in (Bloch) momentum space or Brillouin zone in the search for vanishing group velocities. A comparison of energy curves for some values of η is given in Fig. 3. The time average of the position using expression (25) can be written as

$$\langle x_{ZB} \rangle_\psi = \left\langle \left\{ \frac{i\xi}{2} H'^{-1} [\sigma_x - \xi p_x (H')^{-1}] (e^{-2iH't} - 1) \right\} \right\rangle_\psi. \quad (28)$$

By using the wave-packet decomposition with Fourier coefficients $\psi_{k,s}$, the oscillating part of the expectation value of x is handled according to

$$\begin{aligned} \langle x_{ZB} \rangle_\psi = & -\alpha^2 \xi \sum_s \int_0^\pi dk \frac{k \cos(2E't)}{E'^3} |\psi_{k,s}|^2 \\ & + \sum_{s,s'} \int_0^\pi dk \left[\frac{-i\alpha}{E'} \sin(2E't) (u_2^* u_1 - u_1^* u_2) \right. \\ & \left. + \frac{\alpha^2}{E'^2} \cos(2E't) (u_1^* u_2 + u_2^* u_1) \right] (\psi_{k,s} \psi_{k,s'}^*), \quad (29) \end{aligned}$$

where $E' = s\sqrt{4\xi^2 \sin^2(\frac{k}{2}) + \alpha^2}$. The above expression can be simplified by using the stationary phase approximation at $k = 0, \pi$, as

$$\begin{aligned} \langle x_{ZB} \rangle_\psi & \simeq \sqrt{\frac{\pi}{t\vartheta}} e^{\frac{\pi}{10}} \left[\frac{\alpha^2 \xi \pi \sin(2\omega't)}{\omega'^3} - \frac{\alpha \sqrt{\omega'^2 - \alpha^2}}{\omega'^2} \cos(2\omega't) \right], \quad (30) \end{aligned}$$

where $\omega' = s\sqrt{4\xi^2 + \alpha^2}$ and $\vartheta = \frac{-\xi^4 \pi^2}{\omega'^3} + \frac{\xi^2}{\omega'}$. It is clear that the trembling motion vanishes with an envelope curve of $1/\sqrt{t}$ [64]. We note that the amplitudes and frequencies of the oscillation are independent of the deformation parameter

η . This result is valid only for the Dirac approximation and, in general, the corrections due to η have an impact on $\langle x_{ZB} \rangle$ for the tight-binding system with second neighbors. To see the dependence of the deformation parameter η clearly on the changing shape of the wave packets, we obtain $\langle x^2 \rangle_\psi$ as

$$\begin{aligned} \langle x^2 \rangle_\psi = & e^{-\frac{\pi}{10}} \alpha^2 \omega' + e^{-\frac{\pi}{10}} (\xi^2 \omega' + 12\eta^2 \omega'^2 - 4\alpha\eta\xi\omega')t^2 \\ & - 4e^{-\frac{\pi}{10}} \sqrt{\frac{\pi t}{\vartheta}} \left[-\eta\alpha^2\pi^2\xi \sin(2\omega't) \right. \\ & \left. + \frac{\eta\pi\alpha\sqrt{\omega'^2 - \alpha^2}}{\omega'^2} \cos(2\omega't) \right]. \end{aligned} \quad (31)$$

These results support our previous discussion on wave-packet expansion.

V. CONCLUSIONS

The calculation of an emulation of deformed Dirac equations by means of photonic waveguide arrays with a theoretical study of these equations have been combined. The tight-binding approach to coupling engineering has led to satisfactory results regarding spectrum and wave-function simulations. We have shown how to get around subtle obstacles regarding the correspondence of photonic trembling and relativistic *Zitterbewegung*, as they differ by small but visible amounts when full frequency-band computations are employed. We were able to confirm the η corrections due to algebraic deformations in the evolution of localized wave packets. Interestingly, it was the \sqrt{t} envelope which ultimately carried the deformation, leading to a persistent oscillatory effect in the width and prolonged by an increase proportional to η . All trembling components of the width remained

untouched, including rarely seen, i.e., short-lived but always present, envelope $1/\sqrt{t}$. One important aspect of the κ -deformed Dirac equation is the appearance of an approximately flat band for a large value of η . It is remarkable that by changing the next-nearest-neighbor coupling of microwave resonators, the band becomes flat. We also found a strong dependence on the ballistic part t^2 , controlling the overall speed of expansion, but such an effect already appears in the evolution of scalar particles, as it has little to do with spin. From a technical point of view, we have shown that photonic waveguides may enable experimentalists to study the effects of noncommutative spacetime in the laboratory. We should also comment on a renewed interest in elastic systems due to the flexibility of their experimental setups. The construction of elastic waveguides using aluminum plates makes acoustic transport an attractive area in which emulations may play an interesting role, given the rich phenomenology of vibrational transport using various types of polarizations [65–68]. As we mention above, microwave experiments may also be considered for the realization of the κ -deformed Dirac equation.

ACKNOWLEDGMENTS

P.M. gratefully acknowledges a fellowship from UNAM-DGAPA. J.A.F.-V. acknowledges financial support from CONACYT Project No. A1-S-18696. T.H.S. and P.M. acknowledge financial support from CONACYT Project No. Fronteras 952, CONACYT Project No. 254515, as well as UNAM-DGAPA-PAPIIT Projects No. AG100819 and No. IN113620. We thank F. Leyvraz for useful discussions and comments.

-
- [1] J. Y. Vaishnav and C. W. Clark, Observing *Zitterbewegung* with Ultracold Atoms, *Phys. Rev. Lett.* **100**, 153002 (2008).
 - [2] J. Otterbach, R. G. Unanyan, and M. Fleischhauer, Confining Stationary Light: Dirac Dynamics and Klein Tunneling, *Phys. Rev. Lett.* **102**, 063602 (2009).
 - [3] L. Lamata, J. Leon, T. Schaetz, and E. Solano, Dirac Equation and Quantum Relativistic Effects in a Single Trapped Ion, *Phys. Rev. Lett.* **98**, 253005 (2007).
 - [4] R. Gerritsma, G. Kirchmair, F. Zähringer, E. Solano, R. Blatt, and C. F. Roos, Quantum simulation of the Dirac equation, *Nature (London)* **463**, 68 (2010).
 - [5] P. Majari, A. Luis, and M. R. Setare, Mapping of the 2+1 q-deformed Dirac oscillator onto the q-deformed Jaynes-Cummings model, *Europhys. Lett.* **120**, 44002 (2017).
 - [6] C. Quesne and V. M. Tkachuk, Generalized deformed commutation relations with nonzero minimal uncertainties in position and/or momentum and applications to quantum mechanics, *SIGMA* **3**, 016 (2007).
 - [7] C. Quesne and V. M. Tkachuk, Lorentz-covariant deformed algebra with minimal length, *Czech. J. Phys.* **56**, 1269 (2006).
 - [8] A. Connes, *Noncommutative Geometry* (Academic, San Diego, 1994).
 - [9] I. Hinchliffe, N. Kersting, and Y. L. Ma, Review of the Phenomenology of Noncommutative Geometry, *Int. J. Mod. Phys. A* **19**, 179 (2004).
 - [10] C. Blohmann, Free q-deformed relativistic wave equations by representation theory, *Eur. Phys. J. C* **30**, 435 (2003).
 - [11] B. J. Schroers and M. Wilhelm, Towards non-commutative deformations of relativistic wave equations in 2+1 dimensions, *SIGMA* **10**, 053 (2014).
 - [12] J. A. Franco-Villafañe, E. Sadurní, S. Barkhofen, U. Kuhl, F. Mortessagne, and T. H. Seligman, First Experimental Realization of the Dirac Oscillator, *Phys. Rev. Lett.* **111**, 170405 (2013).
 - [13] E. Sadurní, T. Seligman, and F. Mortessagne, Playing relativistic billiards beyond graphene, *New J. Phys.* **12**, 053014 (2010).
 - [14] S. Bittner, B. Dietz, M. Miski-Oglu, P. Oria Iriarte, A. Richter, and F. Schaefer, Observation of a Dirac point in microwave experiments with a photonic crystal modeling graphene, *Phys. Rev. B* **82**, 014301 (2010).
 - [15] U. Kuhl, S. Barkhofen, T. Tudorovskiy, H.-J. Stoeckmann, T. Hossain, L. de Forges de Parny, and F. Mortessagne, Dirac point and edge states in a microwave realization of tight-binding graphene-like structures, *Phys. Rev. B* **82**, 094308 (2010).
 - [16] B. Dietz and A. Richter, Quantum and wave dynamical chaos in superconducting microwave billiards, *Chaos* **25**, 097601 (2015).
 - [17] B. Dietz and A. Richter, From graphene to fullerene: Experiments with microwave photonic crystals, *Phys. Scripta* **94**, 014002 (2018).

- [18] S. Dehdashti, R. Li, J. Liu, F. Yu, and H. Chen, Realization of non-linear coherent states by photonic lattices, *AIP Adv.* **5**, 067165 (2015).
- [19] A. Rai, C. Lee, C. Noh, and D. G. Angelakis, Photonic lattice simulation of dissipation-induced correlations in bosonic systems, *Sci. Rep.* **5**, 8438 (2015).
- [20] R. A. Sepkhanov, Ya. B. Bazaliy, and C. W. J. Beenakker, Extremal transmission at the Dirac point of a photonic band structure, *Phys. Rev. A* **75**, 063813 (2007).
- [21] S. Longhi, Photonic realization of the relativistic Dirac oscillator, *Opt. Lett.* **35**, 1302 (2010).
- [22] A. Slobozhanyuk, S. H. Mousavi, X. Ni, D. Smirnova, Y. S. Kivshar, and A. B. Khanikaev, Three-dimensional all-dielectric photonic topological insulator, *Nat. Photon.* **11**, 130 (2017).
- [23] M. R. Setare, P. Majari, C. Noh, and Sh. Dehdashti, Photonic realization of the deformed Dirac equation via the segmented graphene nanoribbons under inhomogeneous strain, *J. Mod. Opt.* **66**, 16 (2019).
- [24] S. Longhi, Classical simulation of relativistic quantum mechanics in periodic optical structures, *Appl. Phys. B* **104**, 453 (2011).
- [25] E. Rivera-Mocinos and E. Sadurní, Inverse lattice design an its application to bent waveguides, *J. Phys. A: Math. Theor.* **49**, 175302 (2016).
- [26] P. Russell, *Science* **229**, 358 (2003).
- [27] S. Somekh, E. Garmire, A. Yariv, H. L. Garvin, and R. G. Hunsperger, Channel optical waveguide directional couplers, *Appl. Phys. Lett.* **22**, 46 (1973).
- [28] A. L. Jones, Coupling of Optical Fibers and Scattering in Fibers, *J. Opt. Soc. Am.* **55**, 261 (1965).
- [29] L. Villanueva Vergara and B. M. Rodriguez-Lara, Gilmore-Perelomov symmetry based approach to photonic lattices, *Opt. Express* **23**, 22836 (2015).
- [30] G. Dresselhaus, Spin-Orbit Coupling Effects in Zinc Blende Structures, *Phys. Rev.* **100**, 580 (1955).
- [31] K. Flouris, S. Succi, and H. J. Herrmann, Quantized Alternate Current on Curved Graphene, *Condens. Matter* **4**, 39 (2019).
- [32] G. W. Semenoff, Condensed-Matter Simulation of a Three-Dimensional Anomaly, *Phys. Rev. Lett.* **53**, 2449 (1984).
- [33] C. W. J. Beenakker, Andreev reflection and Klein tunneling in graphene, *Rev. Mod. Phys.* **80**, 1337 (2008).
- [34] M. Ramezani Masir, P. Vasilopoulos, A. Matulis, and F. M. Peeters, Direction-dependent tunneling through nanostructured magnetic barriers in graphene, *Phys. Rev. B* **77**, 235443 (2008).
- [35] L. Dell Anna, P. Majari, and M. R. Setare, From Klein to anti-Klein tunneling in graphene tuning the Rashba spin-orbit interaction or the bilayer coupling, *J. Phys., Condens. Matter* **30**, 415301 (2018).
- [36] Y. Betancur Ocampo, F. Leyvraz, and T. Stegmann, Electron Optics in Phosphorene pn Junctions: Negative Reflection and Anti-Super-Klein Tunneling, *Nano Lett.* **19**, 7760 (2019).
- [37] J. Lukierski, H. Ruegg, and W. J. Zakrzewski, Classical and Quantum Mechanics of Free κ -Relativistic Systems, *Ann. Phys.* **243**, 90 (1995).
- [38] S. Meljanac and M. Stojic, New realizations of Lie algebra kappa-deformed Euclidean space, *Eur. Phys. J. C* **47**, 531 (2006).
- [39] A. Kempf, Quantum group-symmetric Fock spaces with Bargmann-Fock representation, *Lett. Math. Phys.* **26**, 1 (1992).
- [40] J. Lukierski, A. Nowicki, H. Ruegg, and V. N. Tolstoy, q-deformation of Poincaré algebra, *Phys. Lett. B* **264**, 331 (1991).
- [41] M. Daszkiewicz, J. Lukierski, and M. Woronowicz, Towards quantum noncommutative κ -deformed field theory, *Phys. Rev. D*, **77**, 105007 (2008).
- [42] C. A. S. Young and R. Zegers, Covariant particle statistics and intertwiners of the κ -deformed Poincaré algebra, *Nucl. Phys. B* **797**, 537 (2008).
- [43] M. Dimitrijevic, L. Jonke, L. Möller, E. Tsouchnika, J. Wess, and M. Wohlgenannt, Deformed field theory on κ -spacetime, *Eur. Phys. J. C* **31**, 129 (2003).
- [44] S. Majid and H. Ruegg, Bicrossproduct structure of κ -Poincaré group and non-commutative geometry, *Phys. Lett. B* **334**, 348 (1994).
- [45] J. Lukierski, A. Nowicki, and H. Ruegg, New quantum Poincaré algebra and κ -deformed field theory, *Phys. Lett. B* **293**, 344 (1992).
- [46] J. Lukierski and H. Ruegg, Quantum κ -Poincaré in any dimension, *Phys. Lett. B* **329**, 189 (1994).
- [47] S. Doplicher, K. Fredenhagen, and J. E. Roberts, The quantum structure of spacetime at the Planck scale and quantum fields, *Comm. Math. Phys.* **172**, 187 (1995).
- [48] T. R. Govindarajan, K. S. Gupta, E. Harikumar, S. Meljanac, and D. Meljanac, *Phys. Rev. D* **80**, 025014 (2009).
- [49] A. Nowicki, E. Sorace, and M. Tarlini, The quantum deformed Dirac equation from the κ Poincaré algebra, *Phys. Lett. B* **302**, 419 (1993).
- [50] J. Lukierski, H. Ruegg, and W. Rühl, From κ -Poincaré algebra to κ -Lorentz quasigroup. A deformation of relativistic symmetry, *Phys. Lett. B* **313**, 357 (1993).
- [51] E. Harikumar, M. Sivakumar, and N. Srinivas, κ deformed Dirac equation, *Mod. Phys. Lett. A* **26**, 1103 (2011).
- [52] D. Kovacevic, S. Meljanac, A. Pachol, and R. Strajn, Generalized Poincaré algebras, Hopf algebras and kappa-Minkowski spacetime, *Phys. Lett. B* **711**, 122 (2012).
- [53] A. Agostini, G. A. Camelia, and M. Arzano, Dirac spinors for Doubly Special Relativity and κ Minkowski noncommutative spacetime, *Class. Quantum Grav.* **21**, 2179 (2004).
- [54] G. Amelino-Camelia, L. Smolin, and A. Starodubtsev, Quantum symmetry, the cosmological constant and Planck-scale phenomenology, *Class. Quantum Grav.* **21**, 3095 (2004).
- [55] G. Amelino-Camelia, Testable scenario for relativity with minimum length, *Phys. Lett. B* **510**, 255 (2001).
- [56] G. Amelino-Camelia, Gravity-wave interferometers as quantum-gravity detectors, *Nature (London)* **398**, 216 (1999).
- [57] D. J. Gross and P. F. Mende, String theory beyond the Planck scale, *Nuclear Phys. B* **303**, 407 (1988).
- [58] G. Amelino-Camelia, C. Laemmerzahl, F. Mercati, and G. M. Tino, Constraining the Energy-Momentum Dispersion Relation with Planck-Scale Sensitivity Using Cold Atoms, *Phys. Rev. Lett.* **103**, 171302 (2009).
- [59] G. Gubitosi, L. Pagano, G. Amelino-Camelia, A. Melchiorri, and A. Cooray, A constraint on Planck-scale modifications to electrodynamics with CMB polarization data, *J. Cosmol. Astropart. Phys.* **08**, 021 (2009).
- [60] E. Schrödinger, Über die kräftefreie Bewegung in der relativistischen Quantenmechanik, *Sitzungsber. Preuss. Akad. Wiss. Phys. Math. Kl.* **24**, 418 (1930).
- [61] X. Zhang, Observing *Zitterbewegung* for Photons near the Dirac Point of a Two-Dimensional Photonic Crystal, *Phys. Rev. Lett.* **100**, 113903 (2008).

- [62] K. Huang, On the *Zitterbewegung* of the Dirac Electron, *Am. Phys. J* **20**, 479 (1952).
- [63] A. Bermudez, M. A. Martin-Delgado, and A. Luis, Nonrelativistic limit in the 2+1 Dirac oscillator: A Ramsey-interferometry effect, *Phys. Rev. A* **77**, 033832 (2008).
- [64] A. S. Rosado, J. A. Franco-Villafañe, C. Pineda, and E. Sadurní, Stern-Gerlach splitters for lattice quasispin, *Phys. Rev. B* **94**, 045129 (2016).
- [65] K. Hyde, J. Y. Chang, C. Bacca, and J. A. Wickert, Parameter studies for plane stress in-plane vibration of rectangular plates, *J. Sound Vib.* **247**, 471 (2001).
- [66] A. Arreola-Lucas, J. A. Franco-Villafañe, G. Baez, and R. A. Méndez-Sánchez, In-plane vibrations of a rectangular plate: Plane wave expansion modelling and experiment, *J. Sound Vib.* **342**, 168 (2015).
- [67] F. Ramírez-Ramírez, E. Flores-Olmedo, G. Báez, E. Sadurní, and R. A. Méndez-Sánchez, Emulating tightly bound electrons in crystalline solids using mechanical waves, *Sci. Rep.* **10**, 10229 (2020).
- [68] E. Flores-Olmedo, A. M. Martínez-Arguello, M. Martínez-Mares, G. Baez, J. A. Franco-Villafañe, and R. A. Méndez-Sánchez, Experimental evidence of coherent transport, *Sci. Rep.* **6**, 25157 (2016).